0013-7227/99/$03.00/0
Endocrinology

Vol. 140, No. 12
Printed in U.S.A.

Expression and Signal Transduction of Calcium-Sensing Receptors in Cartilage and Bone*

WENHAN CHANG, CHIALING TU, TSUI-HUA CHEN, LASZLO KOMUVES, YUKO ODA, STACY A. PRATT, SCOTT MILLER, AND DOLORES SHOBACK

Endocrine Research Unit (W.C., C.T., T.-H.C., S.A.P., D.S.), Department of Medicine, Department of Dermatology (L.K., Y.O.), Veterans Affairs Medical Center, University of California, San Francisco, California 94121; and Department of Radiobiology (S.M.), School of Medicine, University of Utah, Salt Lake City, Utah 84112

ABSTRACT

We previously showed that Ca^{2+}-sensing receptors (CaRs) are expressed in chondrogenic RCJ3.1C5.18 (C5.18) cells and that changes in extracellular $[Ca^{2+}]$ ($[Ca^{2+}]_o$) modulate nodule formation and chondrogenic gene expression. In the present study, we detected expression of CaRs in mouse, rat, and bovine cartilage and bone by *in situ* hybridization, immunocytochemistry, immunoblotting, and RT-PCR; and we tested the effects of CaR agonists on signal transduction in chondrogenic and osteogenic cell lines. *In situ* hybridization detected CaR transcripts in most articular chondrocytes and in the hypertrophic chondrocytes of the epiphyseal growth plate. Expression of CaR transcripts was weak or absent, however, in proliferating and maturing chondrocytes in the growth plate. In bone, CaR transcripts were present in osteoblasts, osteocytes, and bone marrow cells, but rarely in osteoclasts. A complementary DNA was amplified from mouse growth plate cartilage, which was highly homologous to the human parathyroid CaR sequence. Immunocytochemistry of cartilage and bone with CaR antisera confirmed these findings. Western blotting revealed specific bands (~140–190 kDa) in membrane fractions isolated from growth plate cartilage, primary cultures of rat chondrocytes, and several osteogenic cell lines (SaOS-2, UMR-106, ROS 17/2.8, and MC3T3-E1). InsP responses to high $[Ca^{2+}]_o$ were evident in C5.18 cells and all osteogenic cell lines tested except for SaOS-2 cells. In the latter, high $[Ca^{2+}]_o$ reduced PTH-induced cAMP formation. Raising $[Ca^{2+}]_o$ also increased intracellular free $[Ca^{2+}]$ in SaOS-2 and C5.18 cells. These studies confirm expression of CaRs in cartilage and bone and support the concept that changes in $[Ca^{2+}]_o$ may couple to signaling pathways important in skeletal metabolism. (*Endocrinology* **140:** 5883–5893, 1999)

MOBILIZATION AND DEPOSITION of Ca^{2+} into cartilage and bone matrix are key steps in mineralization (1–3). Studies with vitamin D- and Ca^{2+}-deficient animals demonstrate that Ca^{2+} availability is crucial for normal skeletal development (2, 4). Although Ca^{2+} balance *in vivo* is regulated by circulating hormones, it seems likely that local mechanisms at the tissue level are involved in mobilizing Ca^{2+} from the extracellular fluid into matrix during cartilage and bone formation (2–5).

In vitro studies have demonstrated that extracellular $[Ca^{2+}]$ ($[Ca^{2+}]_o$) influences chondrogenic and osteogenic function. Studies by Bonen and Schmid (6) showed that high $[Ca^{2+}]_o$ increased type II and X collagen synthesis in tibio-tarsus chondrocytes from chick embryos. In the eggshell-less chicken model, Ca^{2+} deprivation induced formation of cartilage nodules in the calvaria, a site at which intramembranous bone typically develops (7). Other studies with this model identified a population of calvarial cells that preferentially differentiated into cartilage when maintained at low $[Ca^{2+}]_o$ (8). Our previous studies showed that changes in $[Ca^{2+}]_o$ modulate matrix protein expression and several functions of the nontransformed chondrogenic C5.18 cells (9). These observations suggest that chondrocytes have the ability to detect and respond to different $[Ca^{2+}]_o$.

Ca^{2+} is known to affect several aspects of bone cell function. Osteoclasts *in vitro* respond to increases in $[Ca^{2+}]_o$ with an elevation of intracellular free $[Ca^{2+}]$ ($[Ca^{2+}]_i$), and high $[Ca^{2+}]_o$ suppresses bone resorption (10, 11). Changes in $[Ca^{2+}]_o$ and CaR agonists modulate DNA synthesis and chemotactic responses in osteoblast-like MC3T3-E1 (12–14) and bone marrow cells (15). The mechanisms underlying this sensitivity to $[Ca^{2+}]_o$ are, however, still unclear.

$[Ca^{2+}]_o$ regulates diverse cellular functions by activating membrane Ca^{2+}-sensing receptors (CaRs) (16, 17). By multiple approaches, we previously found parathyroid-like CaRs in C5.18 cells (9). Other laboratories have reported that CaRs are expressed in bone marrow cells (15), osteoblastic MC3T3-E1 cells (14), the osteosarcoma cell lines UMR-106 and SaOS-2 (18), and cultured rabbit osteoclasts (11).

To date, no information is available regarding which cells express CaRs in cartilage and bone. To address this issue, we performed *in situ* hybridization, immunocytochemistry, and immunoblotting. We also assessed whether CaR agonists could couple to signal transduction pathways in bone and cartilage model systems. CaRs are expressed in specific cells in bone and cartilage, and their expression pattern may provide clues critical to understanding how Ca^{2+} alters skeletal homeostasis.

Received April 7, 1999.
Address all correspondence and requests for reprints to: Dolores Shoback, 111N, Endocrine Research Unit, Veterans Affairs Medical Center, 4150 Clement Street, San Francisco, California 94121. E-mail: dolores@itsa.ucsf.edu.
* This work was supported by a Merit Review from Department of Veterans Affairs, NIH Grant RO1-DK43400, the Academic Senate of the University of California San Francisco, and NIH Grant P01-AR39448.

Materials and Methods

Materials

Culture media were prepared by the Cell Culture Facility of the University of California, San Francisco. Fura-2 AM was from Molecular Probes, Inc. (Eugene, OR). FCS was obtained from Intergen Company (Purchase, NY). ^{3}H-myoinositol was purchased from Amersham Pharmacia Biotech (Arlington Heights, IL). Digoxigenin, RNA polymerase DNA, and DNA polymerase were from Roche Molecular Biochemicals (Indianapolis, IN). Biotinylated tyramide reagent and streptavidin peroxidase were from DAKO Corp. (Carpinteria, CA). Superscript II reverse transcriptase and oligo-dT primers were purchased from Life Technologies (Grand Island, NY). Other reagents were from Sigma (St. Louis, MO), unless otherwise specified.

Tissue preparation

The femurs and tibias from 21-day-old rats were obtained after euthanasia, according to protocols approved by the Animal Welfare Subcommittee of the San Francisco Department of Veteran Affairs Medical Center. The tibia growth plate and adjacent articular cartilage from newborn calves were dissected shortly after death. All tissues were immediately fixed in paraformaldehyde (5%, vol/vol) plus glutaraldehyde (0.2%, vol/vol) at 4 C for 24–48 h and decalcified with EDTA (10%, wt/vol) in PBS at 4 C for 2–3 weeks. After paraffin embedding, 5-μm sections were cut and mounted on glass slides.

Cell culture

C5.18 cells, derived from fetal rat calvaria (19), were provided by Dr. Jane E. Aubin (University of Toronto, Canada) and were maintained as previously described (9). The osteogenic cell lines MC3T3-E1, ROS 17/2.8, UMR-106, and SaOS-2 cells were cultured in α-modified MEM, Ham's F-12 media, DMEM, and McCoy's media, respectively, supplemented with FCS (10%, vol/vol), penicillin (100 U/ml), and streptomycin (100 μg/ml). Measurements of inositol phosphates (InsPs) and cAMP were performed on 1- to 2-day postconfluent cells in 35-mm wells approximately 48–72 h after plating (5×10^4 cells/cm^2) (20–22).

Primary chondrocyte cultures for Western blotting were prepared (23) from articular cartilage from 3-month-old rats, which was aseptically dissected in ice-cold Medium A [D-MEM plus HEPES (20 mM), $NaHCO_3$ (45 mM, pH 7.4), penicillin (100 U/ml), and streptomycin (100 μg/ml)]. After mincing, cartilage pieces were treated with trypsin (0.25%) in Medium A for 30 min at 37 C. After inactivating trypsin with Medium A containing heat-inactivated FCS (10%, vol/vol), tissue was digested in Medium A (5 ml/g tissue) with collagenase IA (0.18 g/100 ml), hyaluronidase (0.1 g/100 ml), and deoxyribonuclease I (0.01 g/100 ml), at 37 C, with gentle agitation. Cells were separated from undigested cartilage with a nylon mesh, collected by centrifugation at $400 \times g$ for 10 min, and washed twice with Medium A. Cells released from cartilage were plated in α-modified MEM, supplemented with nucleosides (0.004%, wt/vol), FCS (15%, vol/vol), penicillin (100 U/ml), and streptomycin (100 μg/ml), for 2 days, to allow for attachment. Chondrocytes were then replated at a density of 5×10^4 cells/cm^2 and allowed to reach confluence before membrane protein isolation.

In situ hybridization

In situ hybridization of bone sections was adapted from previously described methods using digoxigenin-labeled sense or antisense RNA probes (9) prepared from the human keratinocyte CaR complementary (cDNA) template (nucleotides 2442–2746) (24). Signals were visualized with diaminobenzidine (DAB) chromogen substrate. Sections were counterstained with aqueous hematoxylin. Experiments were repeated at least twice on tissue sections from two or more animals.

Immunocytochemistry

Immunocytochemistry of rat articular chondrocytes and bone sections was performed, as previously described (9), with 2 antisera [21825A (500 nM) and no. 421113A (100 nM)] (25). To assess specificity, sections were treated with either antiserum preincubated with excess peptide (100-fold for no. 421113A or 1000-fold for no. 21825A) or nonimmune rabbit IgG. After DAB-staining, cells or sections were counterstained, either with aqueous hematoxylin or with alcian green, for the detection of matrix proteoglycans (9). Experiments were repeated at least four times on tissue sections from two or more animals.

Immunoblotting

Crude membrane protein fractions were prepared (9, 25) from 1- to 2-day postconfluent cultures of rat articular chondrocytes; C5.18, SaOS-2, UMR-106, ROS 17/2.8, and MC3T3-E1 cells; and bovine growth plate cartilage. Immunoblotting was performed after electrophoresis of membrane proteins (50 μg) on 6% SDS-PAGE gels and transfer to nitrocellulose membranes (9, 25). After blocking with Blotto [150 mM NaCl, 10 mM Tris-HCl (pH 7.4), nonfat dry milk (5%, vol/vol), Tween-20 (0.05%, vol/vol)], membranes were incubated with either anti-CaR antiserum (21825A, 50 nM), the same antiserum preincubated with 1000-fold excess peptide, or nonimmune rabbit IgG. After three washes and incubation with peroxidase-conjugated goat antirabbit IgG (Vector Laboratories, Inc., Burlingame, CA; 1:4000), standard ECL assay kits were used for signal detection (Amersham Pharmacia Biotech).

CaR cDNA amplification and subcloning

RT-PCR was performed, as previously described (26), on RNA extracted from epiphyseal growth plate cartilage of 2-day-old mice. Briefly, first-strand cDNA was reverse-transcribed from total RNA using Superscript II reverse transcriptase and oligo-dT primers (26) and subsequently used in PCR with *Pwo* DNA polymerase. Primers were derived from the nucleotide sequence corresponding to the extracellular domain of the mouse kidney CaR cDNA[1] (sense primer: 5′-CAAGGTCATTGTCGTTT TCTCCAGC; antisense primer: 5′-GCAATGCAGGAAGTGTAGTTCTCAT). Amplified cDNA was subcloned into pCR 2.1 plasmid by TOPO-TA cloning kit (Invitrogen, Carlsbad, CA) and sequenced by the Biomolecular Resource Center, University of California, San Francisco.

Measurement of InsPs and cAMP

InsPs were determined in extracts from 1- to 2-day postconfluent C5.18, SaOS-2, UMR-106, ROS 17/2.8, and MC3T3-E1 cells after labeling membrane polyphosphoinositides with ^{3}H-myoinositol (2 μCi/ml) for 48 h, as previously described (25, 27). In each experiment, prelabeled cell cultures were washed three times with MEM and incubated with the same media containing LiCl (10 mM), $CaCl_2$ (0.5 mM), and $MgSO_4$ (0.5 mM) for the pretreatment period. $[Ca^{2+}]_o$ was then varied by adding fresh media containing either 0.5 or 10 mM $CaCl_2$ for 60 min. Total ^{3}H-InsPs were extracted and analyzed as described (25, 27).

Accumulation of cAMP was determined after incubation of cells with assay medium [MEM + BSA (0.1%, wt/vol), IBMX (0.4 mM), $MgSO_4$ (0.5 mM)] containing 0.5, 2.5, 5.0, or 10.0 mM $CaCl_2$ with or without PTH (10^{-6} M) for 10 min (25, 27).

Measurement of $[Ca^{2+}]_i$

$[Ca^{2+}]_i$ was determined in either subconfluent (60–80%) or 1- to 2-day postconfluent C5.18 cells and 1- to 2-day postconfluent SaOS-2 cells using an *InCyt Im2* imaging system (Intracellular Imaging, Inc., Cincinnati, OH) with a 40× Nikon Fluor objective. Briefly, cells were loaded with Fura-2 AM (3–10 μM) in Buffer B [HEPES (20 mM, pH 7.4), NaCl (120 mM), KCl (5 mM), $MgCl_2$ (1 mM), pyruvate (1 mg/ml), glucose (1 mg/ml), and $CaCl_2$ (1.0 mM)] at 37 C for 30–40 min. After three washes with Buffer B, cells were incubated at 37 C for 15–30 min before recording. Fluorescent emission (510 nm) was detected by a COHU high-performance CCD camera (COHU, Inc, San Diego), digitized, and stored in a microcomputer. The 340/380 excitation ratio ($R_{340/380}$) of emitted fluorescence was calculated and presented.

Statistics

Data, normalized to baseline activity in individual experiments, were combined and reported as mean ± SE. Statistical significance was as-

[1] Y. Oda and co-workers, manuscript in preparation; deposited sequence in GenBank (Accession no. AF110178)

sessed by Student *t* test or ANOVA with f-test using Microsoft Corp. Excel (Microsoft Corp., Seattle, WA).

Results

Expression of CaR messenger RNA (mRNA) in cartilage and bone

To assess the expression and distribution of CaR transcripts in rat and bovine cartilage and bone, we performed *in situ* hybridization with a human keratinocyte CaR complementary RNA (cRNA) probe. In growth plate, hybridization signals were present in hypertrophic chondrocytes (Fig. 1, a and c, *arrowheads*). Proliferating chondrocytes demonstrated weaker signals (Fig. 1, a and c, *arrows*). Staining was evident in the majority of articular chondrocytes (Fig. 1b) and was specific, because it was absent when the complementary sense cRNA probe was used (Fig. 1d, and data not shown).

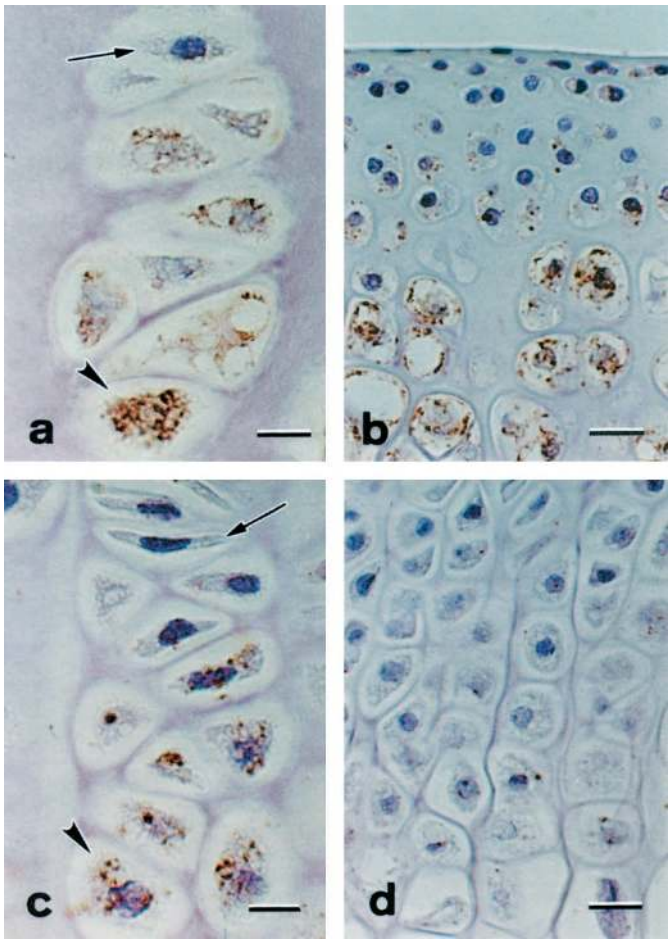

FIG. 1. *In situ* hybridization of CaR transcripts in bovine and rat growth plate cartilage. Hybridization with antisense (a, b, and c) and sense (d) CaR probes was performed as described in *Materials and Methods*. a and c, Expression of CaR transcripts was weak in proliferating (*arrow*) and stronger in hypertrophic chondrocytes (*arrowhead*) in bovine (a) and rat (c) epiphyseal growth plate. b, CaR transcripts were strongly expressed in articular chondrocytes from bovine proximal tibia cartilage. No signals were detected with the CaR sense RNA probe in sections from the epiphyseal growth plate of the rat femur (d) or bovine tibia or rat and bovine articular cartilage (data not shown). Signals were also absent in sections incubated without cRNA probes (data not shown). *Bar*, 10 μm (a and c) and 20 μm (b and d).

In situ hybridization of sections of bovine tibia (Fig. 2a) and rat femur (Fig. 2b) showed expression of CaR transcripts in most osteoblasts (*arrowheads*), osteocytes (*arrows*), and some cells in the bone marrow (*asterisks*). Staining was, however, weak to absent in osteoclasts (Fig. 2, a and b, *double arrowheads*). Staining was judged specific, because it was absent in the hybridization with sense cRNA probe (Fig. 2c).

Immunocytochemical detection of CaRs in cartilage and cultured chondrocytes

To localize CaR proteins by immunocytochemistry, we used an anti-CaR antiserum (421113A) raised against an intracellular epitope of the bovine parathyroid CaR (peptide comprising residues no. 1043–1057) (25). The distribution of CaR protein in cartilage and bone sections was similar to the staining pattern by *in situ* hybridization. In the perichondral area of bovine proximal tibia shown in Fig. 3a, there was strong immunostaining (depicted by *brown color*) in chondroblasts within the chondrogenic layer (*arrows*) but no apparent staining in chondroblasts within the fibrous perichondrium (*asterisk*). Higher magnification confirmed both membrane and cytoplasmic staining in these chondroblasts (Fig. 3b). CaR immunostaining was also evident in the epiphyseal growth plate of the bovine proximal tibia (Fig. 3, c and d). Staining was weak in the proliferating zone (Fig. 3, c and d, *arrows*) and increased as the cells progressed to the maturation (Fig. 3d, *arrowhead*) and hypertrophic zones (Fig. 3c, *arrowhead*; Fig. 3d, *double arrow*). In articular cartilage, staining was strong in chondroblasts and chondrocytes (Fig. 3e, *arrowheads*). CaR immunoreactivity was specific, because staining was not seen when either anti-CaR antiserum preincubated with excess peptide (data not shown) or nonimmune serum was used (Fig. 3f). Identical staining patterns were observed with another anti-CaR antiserum (21825A), raised against an extracellular epitope of the bovine CaR, confirming the above results (data not shown).

Immunocytochemistry of rat distal femur articular cartilage with both CaR antisera demonstrated staining in chondroblasts and chondrocytes on the articular surface (Fig. 4a, and data not shown). The staining patterns with these antisera in the adjacent rat distal femur growth plate were comparable with those noted in Fig. 3 for bovine proximal tibia. Lower-power views showed weak staining in the columns of proliferating cells (Fig. 4b) that increased in hypertrophic chondrocytes (Fig. 4b, *arrow*). This was confirmed in high-power views (Fig. 4c). The specificity of the staining pattern was confirmed by its abolition after preincubation of antiserum with excess peptide (data not shown).

CaRs were present in primary cultures of rat articular chondrocytes, as evidenced by immunostaining within and outside nodules in these cultures, which were identified by alcian green staining (Fig. 5a). CaR staining was more intense in cells within the nodules and absent in cultures incubated with nonimmune IgG (Fig. 5b), underscoring specificity of the staining.

CaR expression in bone

Figure 6a shows the primary spongiosa of bovine tibia in which CaR immunoreactivity is present in most osteoblasts

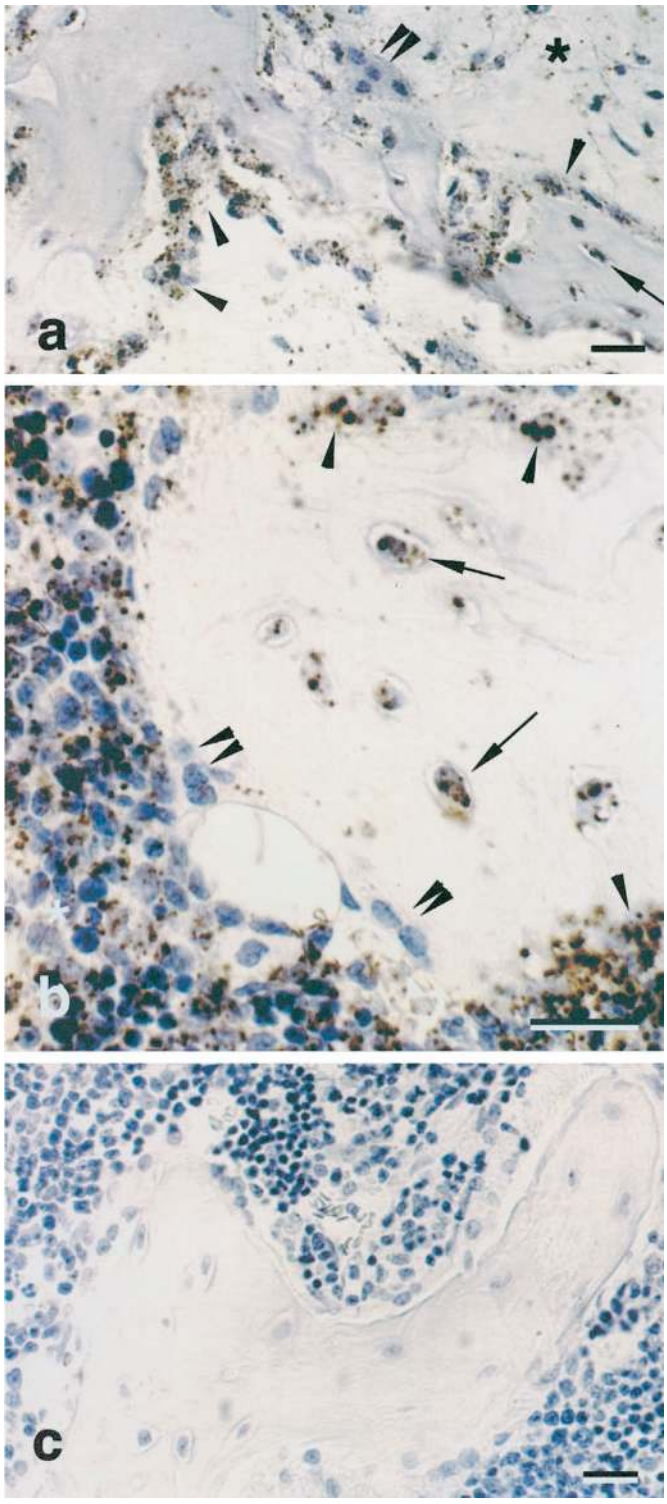

FIG. 2. *In situ* hybridization of CaR transcripts in bone from bovine tibia (a) and rat femur (b and c). Hybridization with antisense (a and b) and sense (c) CaR probes was performed as described in *Materials and Methods*. a and b, Expression of CaR transcripts was evident in osteoblast (*arrowheads*), osteocytes (*arrows*), and cells in bone marrow (*). Staining was weak to absent in osteoclasts (*double arrowhead*). c, No signals were detected with the CaR sense RNA probe in sections from the rat femur or bovine tibia (data not shown). *Bar*, 20 μm.

(*arrowheads*). Staining was comparable, in intensity, with adjacent hypertrophic chondrocytes (*arrows*). There was no immunoreactivity in cells with an osteoclastic or chondroclastic morphology (*double arrowheads*). Higher-power micrographs in Fig. 6b confirmed the cytoplasmic and membrane distribution of the staining in osteoblasts (*arrowheads*) and lack of staining in osteoclasts (*double arrowheads*). In the same field, some mononuclear bone marrow cells (*arrows*) were faintly stained. CaR immunoreactivity was also detected in most osteocytes (Fig. 6c, *arrows*) at levels similar to those of adjacent osteoblasts (Fig. 6c, *arrowheads*).

Although CaR staining was generally absent in osteoclasts (Fig. 6, a–c, *double arrows*), some osteoclasts, farther away from the growth plate, stained positively with anti-CaR antiserum. The intensity of staining in a large osteoclast in Fig. 6d (*arrow*) was comparable with that of adjacent osteoblasts (*arrowheads*). Staining was weak to absent, however, in three smaller osteoclasts in the same field (*double arrows*). CaR expression in osteoclasts may vary, therefore, with their location in bone and perhaps their stage of differentiation, given that the large osteoclasts tend to be older than small osteoclasts.

In rat tibia shown in Fig. 6e, CaR immunoreactivity was detected in osteoblasts (*arrowheads*), cells in the bone marrow, and osteocytes (*arrows*) but not in osteoclasts (*double arrowheads*), confirming the above observations in bovine bone sections. Some osteocytes in the same field were not stained (*double arrows*). Specificity of staining in both bovine and rat tissues was confirmed by its abolition after preincubation of antiserum with excess peptide (data not shown).

Detection of CaR protein by immunoblotting

To assess the size of CaRs, we immunoblotted crude membrane fractions from cultured rat articular chondrocytes, C5.18 cells, bovine growth plate cartilage, and four osteoblastic cell lines. Antisera blotted three major bands in membrane preparations from HEK-293 cells expressing the bovine CaR cDNA (Fig. 7a, *upper panel*, lane 1), as previously observed (9, 25). Bands of approximately 140 and approximately 160 kDa in CaR-expressing HEK-293 cells are thought to be the variably glycosylated forms of the CaR, which has a protein core of approximately 120 kDa (16, 25). The protein band of more than 205 kDa in these membranes is specific and likely represents receptor aggregates (16, 25).

C5.18 cell membrane fractions contain a major band of approximately 150 kDa and two faint bands of sizes approximately 180 and approximately 190 kDa (Fig. 7a, *upper panel*, lane 2) (9). Specific immunoreactivity, larger than our highest protein standard, was also detected in these cells. In rat articular chondrocytes, the most prominent band was approximately 155 kDa (Fig. 7a, *upper panel*, lane 3), although there were several less discrete, but specific, bands between approximately 170 and approximately 200 kDa and more than 205 kDa. In lysates from bovine growth plate cartilage, there was a predominant band of approximately 140 kDa and 2 fainter bands of approximately 168 and approximately 175 kDa (Fig. 7a, *upper panel*, lane 4). Immunoreactivity in these cells was specific, because it was absent when preimmune serum was used and was abolished by preincubation of

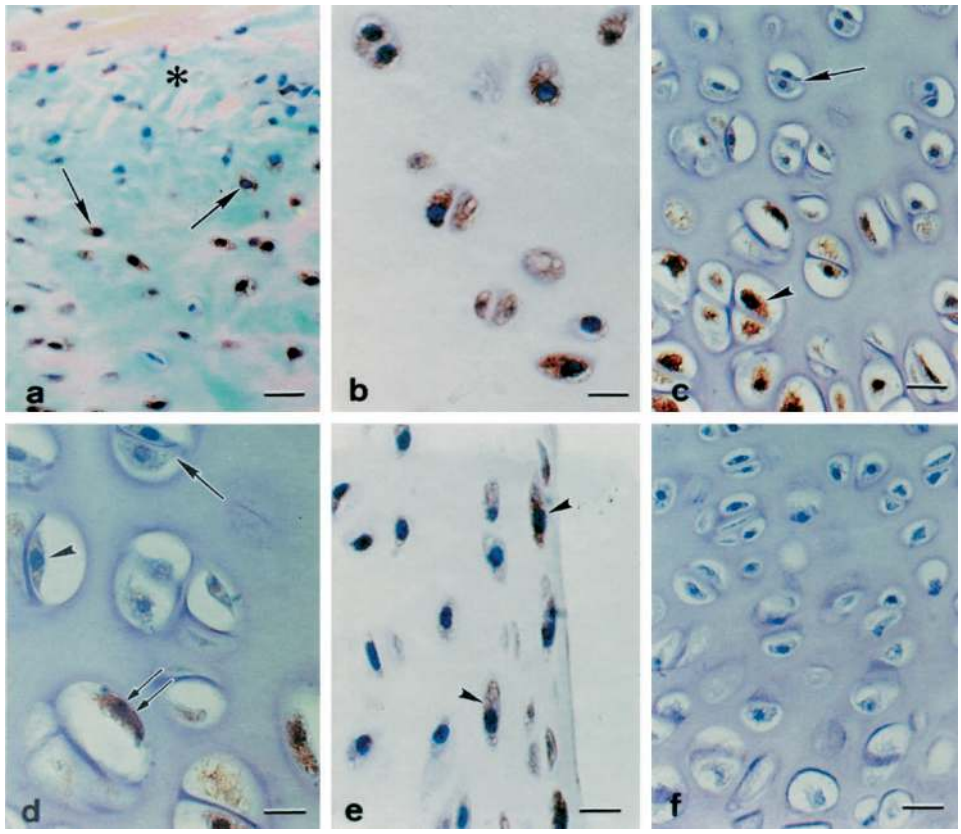

FIG. 3. Immunocytochemical detection of CaRs in bovine articular and growth plate cartilage. Immunocytochemistry with antiserum 421113A (25) was performed as described in *Materials and Methods*. a, The perichondral region of the proximal tibial growth plate, visualized under polarized light, shows the pattern of birefringence of the collagen filament (*pink*) insertions into the fibrous perichondrium (*) and the underlying chondrogenic perichondrium. DAB staining, indicative of CaRs, was detected in chondrocytes (*arrows*) in this region. b, Higher-power micrograph of the tibial growth plate region in panel a, illustrating CaR staining in chondroblasts. c, CaR staining of cells in transition from the proliferating and maturing chondrocyte region to the hypertrophic zone in the tibial growth plate. Faint staining is evident in the proliferating zone (*arrow*), and greater staining is present as the cells mature and hypertrophy (*arrowhead*). d, Higher-power view of the increased CaR staining as proliferating chondrocytes (*arrow*) mature (*arrowhead*) and hypertrophy (*double arrow*). e, CaR staining in chondrocytes located at the tibial articular surface (*arrowheads*). f, Section of growth plate stained with nonimmune rabbit antisera. *Bar*, 20 μm (a, c, e, and f) and 10 μm (b and d).

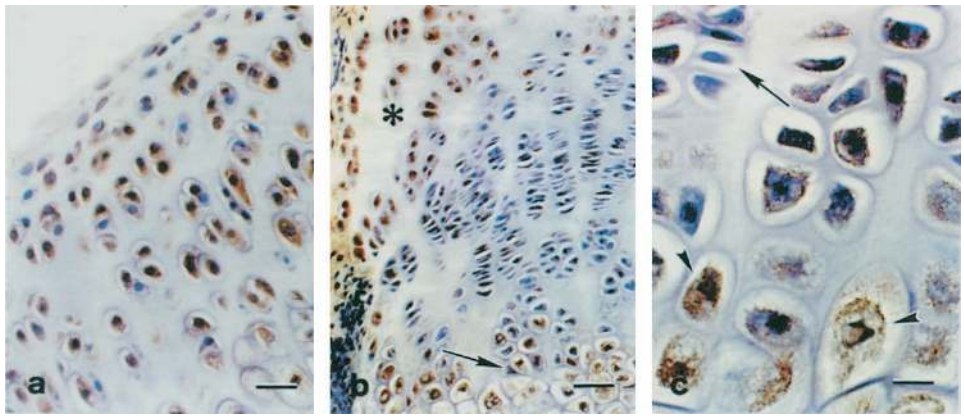

FIG. 4. Immunocytochemical detection of CaRs in rat distal femur articular and growth plate cartilage. a, Articular surface of the distal femur illustrating CaR staining in most chondroblasts near the surface and in chondrocytes in deeper layers of the articular cartilage. b, Lateral perichondral region of the epiphyseal growth plate of the distal femur. Staining for CaR is substantial in the chondrogenic layer of the perichondral collar (*). Proliferating chondrocytes are lightly stained, if at all. Staining is much more evident in hypertrophic chondrocytes (*arrow*). c, Higher-power micrograph of the distal epiphyseal growth plate illustrating weak staining in proliferating chondrocytes (*arrow*) and stronger staining for CaRs in the hypertrophic zone (*arrowheads*). *Bar*, 20 μm (a and b) and 10 μm (c).

antiserum with excess peptide (Fig. 7a, *lower panel*). These results suggest that CaRs in articular chondrocytes and growth plate share epitopes with the bovine parathyroid CaR and are likely to be glycoproteins of similar molecular weight.

In cultured osteoblastic model systems, such as SaOS-2 cells, we detected a prominent band at approximately 190 kDa, a fainter band of approximately 158 kDa, and two bands of more than 200 kDa in membrane fractions (Fig. 7b, *upper panel*, lane 1). A similar pattern was observed in membrane fractions prepared from MC3T3-E1 cells, with one band at approximately 155 kDa, a weaker signal at approximately 190 kDa, and the strongest signal at more than 205 kDa (Fig. 7b, *upper panel*, lane 3). In contrast, we detected only one band of approximately 150 kDa in ROS 17/2.8 cells (Fig. 7b, *upper panel*, lane 2). Two protein bands of approximately 140 and approximately 150 kDa were detected in UMR-106 membrane fractions. The immunoreactivity of the above bands

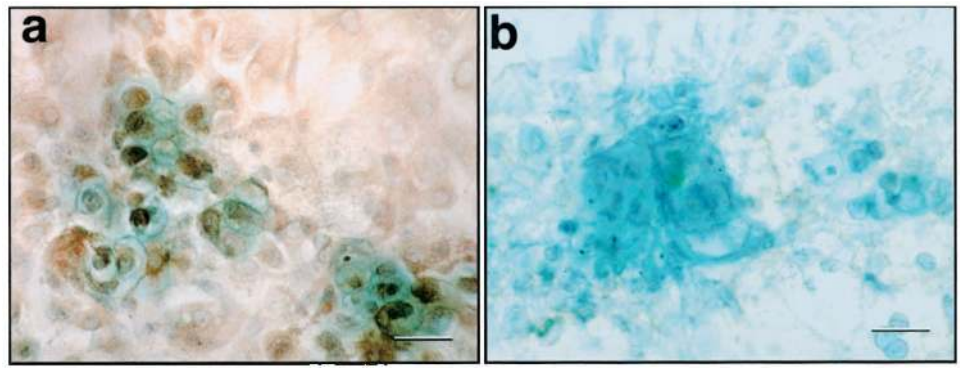

FIG. 5. Expression of CaRs in cultured rat tibial articular chondrocytes. Chondrocytes were incubated with antiserum 21825A (a) or nonimmune serum (b) followed by secondary antibody and then counter-stained with alcian green for the detection of matrix proteoglycans and hematoxylin, as described in *Materials and Methods*. CaRs were expressed in most cells, and immunoreactivity was more intense in the nodules (a). Controls treated with nonimmune serum were negative (b). *Bar*, 20 μm.

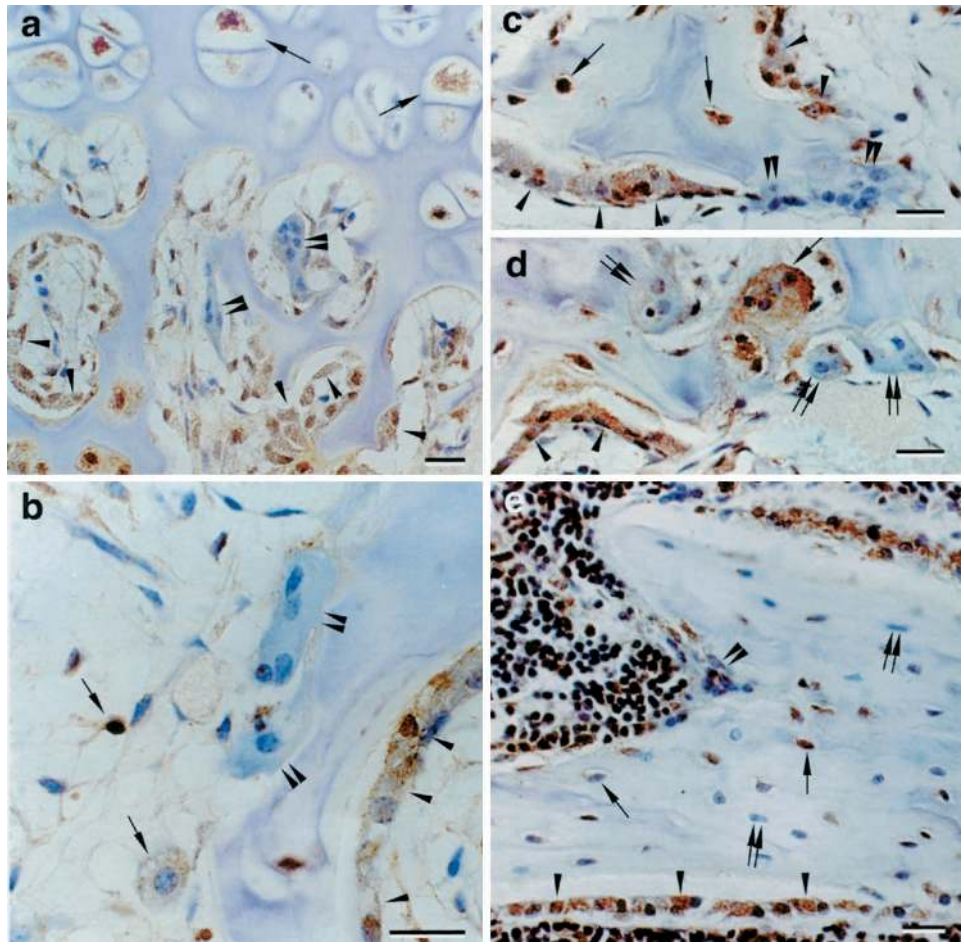

FIG. 6. Immunocytochemistry of bovine and rat bone. Sections were prepared, and CaRs were localized with antiserum 21825A, as described in *Materials and Methods*. a, Primary spongiosa of bovine proximal tibia illustrating diffuse CaR expression in osteoblasts (*single arrowheads*) in the vicinity of hypertrophic chondrocytes (*arrows*). In this region, there was little staining of osteoclasts (*double arrowheads*). b, Higher-power micrograph of the primary spongiosa showing the lack of CaR expression in osteoclasts (*double arrowheads*), weak staining in bone marrow cells (*arrows*), and strong diffuse staining in adjacent layers of osteoblasts (*arrowheads*). c, Secondary spongiosa of bovine proximal tibia illustrating CaR expression in osteocytes in the matrix (*arrows*) of intensity comparable with that in nearby osteoblasts (*arrowheads*). Immunostaining was not detected in osteoclasts in these sections (*double arrows*). d, Sections of secondary spongiosa distal to the growth plate showing four osteoclasts with varying degrees of staining. The largest one (*arrow*) is stained to a degree comparable with that of the adjacent osteoblasts (*arrowheads*). Smaller osteoclasts (*double arrows*) showed weak or absent staining for CaRs. e, Secondary spongiosa of rat tibia showing immunostaining of bone marrow cells, osteoblasts (*arrowheads*), and osteocytes (*arrows*). Osteoclasts (*double arrowheads*) and some osteocytes (*double arrows*) showed weak or absent staining. *Bar*, 20 μm.

was specific, because it was abolished by preincubation of antiserum with excess peptide (Fig. 7b, *lower panels*).

Cloning of a partial CaR cDNA from epiphyseal growth plate cartilage

To determine the molecular identity of a putative CaR in cartilage, we performed RT-PCR on RNA isolated from mouse epiphyseal growth plate and kidney (the latter as a control tissue). A cDNA with an expected size of approximately 1 kb was amplified from both cartilage and kidney (see Fig. 8). The PCR reaction was specific, because no cDNA was amplified from control RNA samples incubated without reverse transcriptase. We subcloned this PCR product and analyzed its sequence. Both the nucleotide and deduced amino acid sequences have a high degree of similarity (89% and 95%, respectively) to the extracellular domain (residues no. 265–599) of the human parathyroid CaR (28), suggesting that this CaR cDNA is the cartilage homologue of the CaRs identified in other systems.

Signal transduction responses to CaR agonists

CaRs couple to polyphosphoinositide turnover, suppression of cAMP accumulation, increases in $[Ca^{2+}]_i$, and stimulation of cation influx in other systems (25, 29). We tested

whether changes in $[Ca^{2+}]_o$ could activate signal transduction pathways in chondrogenic and osteogenic cells. Raising $[Ca^{2+}]_o$ from 0.5 to 10 mM modestly, but significantly, increased InsPs accumulation, by 89 ± 7% in C5.18 cells and to a lesser extent in MC3T3-E1, ROS 17/2.8, and UMR-106 cells, respectively (see Table 1). This increment in $[Ca^{2+}]_o$, however, had no significant effect on InsP production in SaOS-2 cells (see Table 1).

CaRs in parathyroid cells (30), renal cells (31), and HEK-293 cells (25) can also couple to the suppression of cAMP accumulation. Because PTH increases cAMP formation in SaOS-2 (32) and C5.18 cells (19), we examined whether high $[Ca^{2+}]_o$ could suppress PTH-induced cAMP production in these cells. In the absence of PTH, raising $[Ca^{2+}]_o$ from 0.5 to 2.5, 5.0, and 10.0 mM increased cAMP levels, from 4.4 ± 0.8 to 4.7 ± 0.6, 5.2 ± 0.7, and 6.4 ± 0.9 pmol/well, respectively [see Fig. 9, table (n = 12); $P > 0.1$ for 2.5 and 5 mM Ca^{2+} *vs.* controls; and $P < 0.03$ for 10 mM Ca^{2+} *vs.* controls]. Incubation of SaOS-2 cells with PTH (10^{-6} M) at 0.5 mM Ca^{2+} profoundly increased cAMP accumulation, by 16.5 ± 1.1-fold over basal ($P < 0.001$; see Fig. 9). PTH increased cAMP levels by 12.4 ± 1.3, 10.7 ± 1.1, and 9.3 ± 0.7-fold at 2.5, 5.0, and 10 mM Ca^{2+}, respectively (Fig. 9). The ability of PTH to stimulate cAMP accumulation was modestly blunted by raising $[Ca^{2+}]_o$. Similar inhibitory effects of high $[Ca^{2+}]_o$ on cAMP production were also observed in C5.18 cells (data not shown). These findings suggest that the cAMP responses of osteoblastic and chondrogenic cells to PTH can be modulated by the $[Ca^{2+}]_o$.

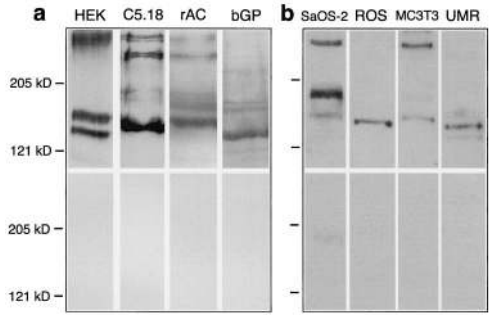

FIG. 7. Immunoblotting of membrane proteins with anti-CaR antiserum. Crude membrane fractions, prepared from 1- to 2-day postconfluent (a) HEK-293 cells stably expressing bovine parathyroid CaRs (HEK) (25), C5.18 cells, rat articular chondrocytes (rAC), and bovine tibia growth plate (bGP) and (b) the osteoblastic cell lines SaOS-2, ROS 17/2.8 (ROS), MC3T3-E1 (MC3T3), and UMR-106 (UMR). Blotting was performed with antiserum 21825A (*upper panels*) or with the same antiserum preincubated with 1000× excess peptide (*lower panels*), as described in *Materials and Methods*.

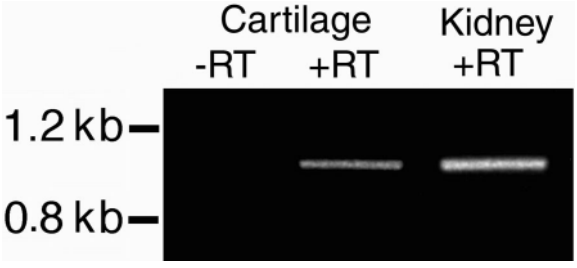

FIG. 8. RT-PCR was performed on RNA isolated from newborn mouse growth plate cartilage and kidney in the presence (+RT) or absence (−RT) of reverse transcriptase, as described in *Materials and Methods*. A CaR cDNA (~1 kb) was amplified from cartilage, and its sequence was analyzed and deposited in GenBank database (accession no. AF159565).

In parathyroid cells, activation of CaRs elevates $[Ca^{2+}]_i$ by releasing Ca^{2+} from intracellular stores and by increasing membrane Ca^{2+} influx (29). We, therefore, measured $[Ca^{2+}]_i$ to test whether high $[Ca^{2+}]_o$ induces Ca^{2+} mobilization in SaOS-2 and C5.18 cells. In SaOS-2 cells, raising $[Ca^{2+}]_o$ from 0.5 to 5 mM induced a gradual increase in $[Ca^{2+}]_i$, which was sustained for more than 10 min. Similar responses were observed in most cells. To test whether PTH could also mediate Ca^{2+} mobilization, cells were treated with PTH (10^{-6} M) before and after raising $[Ca^{2+}]_o$. As shown in Fig. 10, PTH did not affect high $[Ca^{2+}]_o$-stimulated Ca^{2+} mobilization (a) or basal $[Ca^{2+}]_i$ at 0.5 mM Ca^{2+} (b). These and the above observations indicate that signaling pathways coupled to PTH receptors and CaRs differ.

High $[Ca^{2+}]_o$ also increased Ca^{2+} mobilization in C5.18 cells. In subconfluent cell cultures, increasing $[Ca^{2+}]_o$ from 0.5 to 5 mM elevated $[Ca^{2+}]_i$, and two distinct responses were evident (Fig. 11). In approximately 20% of cells, high $[Ca^{2+}]_o$ induced a rapid (within 20 sec) and transient (duration, <180 sec) peak increase in $[Ca^{2+}]_i$. This was followed by a sustained elevation in $[Ca^{2+}]_i$ lasting more than 10 min (Fig. 11a). In the majority of cells (~80%), $[Ca^{2+}]_i$ rose slowly over approximately 2 min, until it reached a plateau, which was sustained for at least 10 min (Fig. 11b). Figure 11c shows the composite kinetics of the changes in $[Ca^{2+}]_i$ recorded from 31 cells in which the sharp initial phase of the response is not evident (n = 3 experiments). In contrast, in 1- to 2-day postconfluent cells, more cells (≥60%) expressed a fast transient intracellular Ca^{2+} response. As a result, the sharp transient phase of the response was more evident in the ensemble recording of the cell populations (Fig. 11d). To determine whether changes in $[Ca^{2+}]_i$ are sensitive to $[Ca^{2+}]_o$ within the physiological range, we performed dose-response studies. Raising $[Ca^{2+}]_o$ from 0.5 to ≥1.0 mM substantially increased $[Ca^{2+}]_i$ (see Fig. 11e), suggesting that physiologic levels of

TABLE 1. Increases in total InsPs caused by high $[Ca^{2+}]_o$

	C5.18	MC3T3-E1	ROS 17/2.8	UMR-106	SaOS-2
% Increase	89 ± 7 (399 ± 20)	46 ± 9 (1852 ± 199)	56 ± 7 (633 ± 82)	62 ± 17 (2088 ± 22)	5 ± 7 (488 ± 57)
P	<0.001	<0.001	<0.001	<0.003	>0.6

InsP production was determined in cells treated with either 0.5 or 10 mM Ca^{2+}, as described in *Materials and Methods*. Net increases in InsP production, when $[Ca^{2+}]_o$ was increased from 0.5 to 10 mM Ca^{2+}, were normalized to the value determined at 0.5 mM Ca^{2+} and expressed as percent increase. *Parentheses* indicate average basal InsP accumulation (cpm/well) at 0.5 mM Ca^{2+}, determined from three independent experiments in triplicate. *P*-values were determined using Student's *t* test.

extracellular Ca^{2+} could readily modulate $[Ca^{2+}]_i$ in these cells. Similar results were obtained in 2 other experiments.

Ca^{2+} entry plays an important role in the sustained phase of high $[Ca^{2+}]_o$-induced Ca^{2+} mobilization in parathyroid cells (29). To test whether Ca^{2+} influx plays a role in C5.18 cells, we examined the effects of the cation channel blockers La^{3+} and Gd^{3+} on intracellular Ca^{2+} responses to high $[Ca^{2+}]_o$. As shown in Fig. 11f, $LaCl_3$ (100 μM) promptly and profoundly suppressed the sustained increase of $[Ca^{2+}]_i$ caused by high $[Ca^{2+}]_o$. $GdCl_3$ (100 μM) produced effects similar to those of $LaCl_3$ (data not shown). These results suggest that high $[Ca^{2+}]_o$ elevates $[Ca^{2+}]_i$ in C5.18 cells by increasing Ca^{2+} uptake across the membrane.

$[Ca^{2+}]_o$, mM	0.5	2.5	5.0	10.0
basal cAMP pmoles/well	4.4 ± 0.8	4.7 ± 0.6	5.2 ± 0.7	6.4 ± 0.9

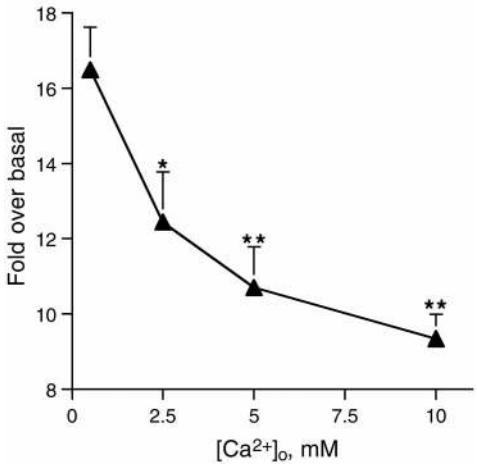

FIG. 9. Inhibition of PTH-induced cAMP production by high $[Ca^{2+}]_o$ in SaOS-2 cells. cAMP content was determined in extracts from cells treated with or without PTH (10^{-6} M) for 10 min at room temperature in the presence of 0.5, 2.5, 5.0, or 10 mM Ca^{2+}. The ability of PTH to induce cAMP production at each $[Ca^{2+}]_o$ was assessed by comparing the cAMP levels, in the presence of PTH, with the basal levels shown in the table, and is presented as fold-increase above basal. *, $P < 0.03$; **, $P < 0.001$, compared with the response at 0.5 mM Ca^{2+}.

Discussion

Cartilage and bone formation require the deposition of Ca^{2+} and other minerals into the extracellular matrix (1, 3). Thus, these tissues must be capable of transporting Ca^{2+} rapidly and quantitatively. Because of this, it is reasonable to hypothesize that these tissues can sense changes in $[Ca^{2+}]_o$. Our previous studies (9) explored the idea that chondrogenic functions are regulated by changes in $[Ca^{2+}]_o$. We found that CaRs, homologous to those in parathyroid and kidney (17), were expressed in chondrogenic C5.18 cells. Because bone and cartilage have many cell types and a highly organized tissue architecture, these studies examined the expression and localization of CaRs in bone and articular and growth plate cartilage and the ability of high $[Ca^{2+}]_o$ to couple to classical signal transduction pathways activated by CaRs. Our findings support the idea that CaRs are differentially expressed in specific cells in bone and cartilage and that this localization may ultimately provide a clue to the functions served by these receptors.

These studies are the first to demonstrate CaR expression in growth plate in a distinctive pattern. Expression is strong in chondroblasts and hypertrophic chondrocytes and absent to weak in proliferating and maturing chondrocytes. This may be important because chondroblasts and hypertrophic chondrocytes serve very different functions. Chondroblasts synthesize matrix proteins, such as proteoglycans and type II collagen, which comprise early hyaline cartilage (3). Hypertrophic chondrocytes, in contrast, participate in later steps of chondrogenesis. They synthesize type X collagen, express alkaline phosphatase, produce matrix vesicles, and accumulate Ca^{2+} in their intracellular compartments (3, 33, 34). These and other steps lead to the mineralization of cartilage and ultimately to new bone formation (1, 3, 33, 35).

Variable expression of CaRs in different populations of chondrocytes may occur because $[Ca^{2+}]_o$ is important to some (but not all) chondrocytes. $[Ca^{2+}]_o$ is likely to be relevant to hypertrophic chondrocytes, which sequester Ca^{2+} and secrete matrix proteins that eventually become mineralized. Perhaps $[Ca^{2+}]_o$ may be less important to the functions of proliferating and maturing chondrocytes in which we found weaker CaR expression. Alternatively, Ca^{2+}-sensing mechanisms other than the CaR may be present in those cells.

Our findings suggest that CaRs may play a role in the

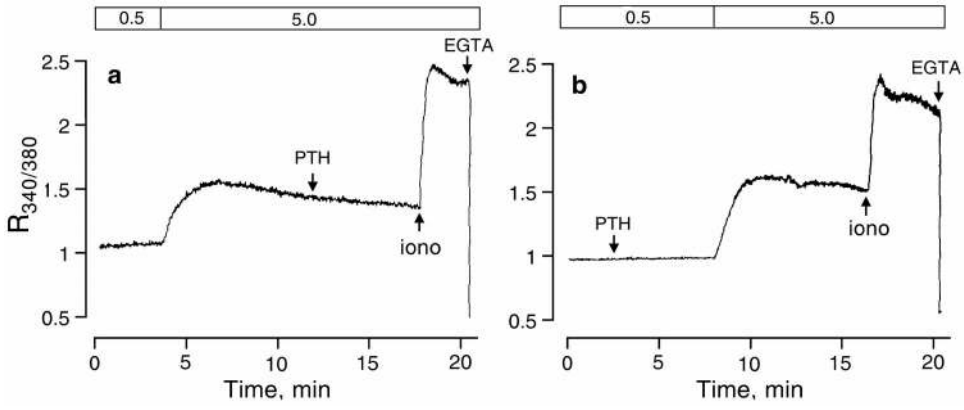

FIG. 10. Intracellular Ca^{2+} responses to changes in $[Ca^{2+}]_o$ and PTH treatment in SaOS-2 cells. $[Ca^{2+}]_i$ was determined as described in *Materials and Methods* in confluence with 1-day postconfluent cells. Data are presented as the values of the ratio of fluorescence at excitation of 340 and 380 nm ($R_{340/380}$). *Horizontal bars on top of the panels* indicate the $[Ca^{2+}]_o$ (in mM) during the recordings. In these experiments, PTH (10^{-6} M) was added either after (a) or before (b) raising $[Ca^{2+}]_o$ from 0.5 to 5.0 mM. Ionomycin (50 μM) and EGTA (20 mM) were added to obtain maximal and minimal $R_{340/380}$, respectively. Data were from 33 cells (a) and 34 cells (b) and are representative of 3 cell preparations.

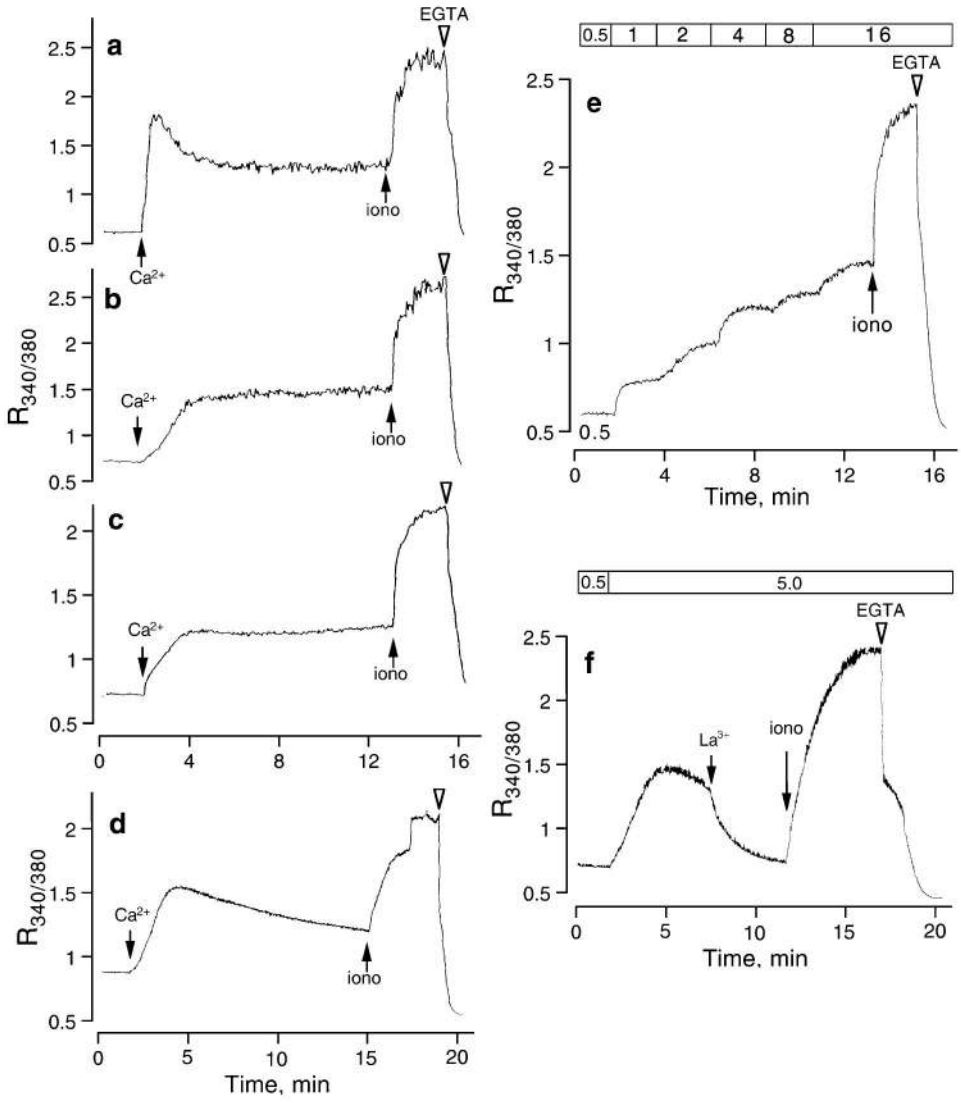

FIG. 11. Intracellular Ca^{2+} responses to changes in $[Ca^{2+}]_o$ in C5.18 cells. Measurements were made in either subconfluent (a, b, c, and e) or 1- to 2-day postconfluent (d and f) cells. a, b, c, and d, Changes of $R_{340/380}$ in response to raising $[Ca^{2+}]_o$ from 0.5 to 5 mM. a and b, Recordings were collected from two representative cells that displayed the different intracellular Ca^{2+} responses in the same experiment. c, Ensemble recordings were made from a population of 31 cells, including those shown in a and b. d, Ensemble recordings were collected from a population of 34 postconfluent cells. e, Intracellular Ca^{2+} responses to raising $[Ca^{2+}]_o$ stepwise from 0.5 to 16 mM. Increments in $[Ca^{2+}]_o$ were made at intervals of 2–3 min, indicated by the *top bar*. The *tracing* represents the ensemble recordings of 28 cells. f, Effect of La^{3+} on the intracellular Ca^{2+} responses to raising $[Ca^{2+}]_o$. $LaCl_3$ (100 μM) was added approximately 5–7 min after raising $[Ca^{2+}]_o$ from 0.5 to 5.0 mM. The tracing represents the ensemble recordings from 35 cells. These data are representative of 3 cell preparations. *Bars over panels e and f* represent $[Ca^{2+}]_o$ in mM.

differentiation of or matrix production by chondrocytes. We previously found that C5.18 cells [which resemble hypertrophic chondrocytes by their expression of late chondrogenic markers (*e.g.* type X collagen and alkaline phosphatase)] respond to high $[Ca^{2+}]_o$. High $[Ca^{2+}]_o$ suppresses aggrecan, type II and type X collagen, and alkaline phosphatase mRNA levels and inhibits cartilage matrix production (9). We also found that high $[Ca^{2+}]_o$ promotes matrix mineralization and the expression of type I collagen, osteonectin, and osteopontin mRNA in C5.18 cells[2] [markers typically associated with the terminal differentiation of hypertrophic chondrocytes (36, 37)]. Thus, CaRs may participate in as-yet-undefined ways in differentiation and mineralization of chondrocytes.

Our studies revealed distinct kinetic patterns of intracellular Ca^{2+} responses in C5.18 cells. There was a fast, transient phase in the intracellular Ca^{2+} response analogous to CaR receptor-mediated Ca^{2+} mobilization in other systems. This response is thought to be caused by the release of Ca^{2+} from intracellular stores (38). This transient Ca^{2+} mobilization was observed in only a small number of cells in subconfluent cultures but became the prevalent response in confluent and postconfluent cultures. It is still unclear how the stage of growth in culture can affect signal transduction responses.

Previous studies did not demonstrate significant changes in CaR expression in C5.18 cells in subconfluent and up-to-10-days postconfluent cultures (9). It is, therefore, likely that the intracellular Ca^{2+} responses we observed at different stages of confluence are caused by postreceptor signaling molecules or possibly to other Ca^{2+}-sensing mechanisms.

Increases in $[Ca^{2+}]_i$, with or without a preceding rapid transient, were sustained for more than 10 min. This prolonged mobilization of Ca^{2+} could be blocked by La^{3+} and Gd^{3+} (suggesting that Ca^{2+} entry via membrane channels is important in sustained Ca^{2+} mobilization). CaRs couple to nonselective cation channels, permeable to Ca^{2+}, in other cells (39). During cartilage differentiation, chondrocytes actively mobilize and store Ca^{2+} in their intracellular compartments, which is later released for matrix mineralization (5, 34). Whether increased CaR expression in hypertrophic chondrocytes amplifies the ability of cells to mobilize and

[2] W. Chang and D. Shoback, unpublished observations.

store Ca^{2+} and produce mineralized cartilage is yet to be explored. As in C5.18 cells, high $[Ca^{2+}]_o$ also induced a sustained increase in $[Ca^{2+}]_i$ in osteoblastic SaOS-2 cells. Because osteoblasts are important in bone matrix synthesis and mineralization, their ability to detect and mobilize Ca^{2+} could be crucial in maintaining mineral homeostasis.

Our findings in rat and bovine bone sections were predictable, in part, by previous studies. CaRs were expressed in most osteoblasts and bone marrow cells and in some (but not all) osteocytes. Studies with RT-PCR and Western and Northern blotting demonstrated CaR expression in UMR-106, SaOS-2, and MC3T3-E1 cells (14, 18). House *et al.* (15) also showed CaR expression in cultured human bone marrow mononuclear cells. Whereas the latter cells may be the precursors of osteoblasts and osteoclasts, the remainder of the studies from other groups were done with transformed osteoblastic (osteosarcoma) cell lines maintained in long-term culture. How closely they resemble normal osteoblasts is uncertain. Our studies are the first to identify CaRs by immunocytochemistry and *in situ* hybridization in normal bone. The fact that high $[Ca^{2+}]_o$ can activate signal transduction pathways in osteoblastic and chondrogenic cell lines, similar to those coupled to classical CaRs, suggests that these receptors may serve similar Ca^{2+}-sensing functions in these systems.

In SaOS-2 cells, increases in $[Ca^{2+}]_o$ produce dual effects on cAMP metabolism. In the absence of PTH, high $[Ca^{2+}]_o$ modestly increased cAMP production. In contrast, high $[Ca^{2+}]_o$ suppressed cAMP production in the presence of PTH. The difference could be caused by the ability of adenylate cyclases to be activated by high $[Ca^{2+}]_i$ (40, 41) in the absence of PTH and the ability of PTH to couple to $G\alpha_s$ and to $G\alpha_i$ activation. Further studies will be needed to address these possibilities definitively.

The distribution of CaRs among osteoclasts was unexpected. CaR immunoreactivity was absent in osteoclasts close to the growth plate but was apparent in osteoclasts in the secondary spongiosa distal to the growth plate. In the secondary spongiosa, the intensity of CaR staining seemed to increase with osteoclast size (see Fig. 4d). Osteoclasts are preferentially formed in the primary spongiosa during bone growth (42), and their age is estimated to be greater as a function of their distance from growth plate (43). Thus, CaR expression may be restricted to the mature osteoclasts. This finding requires confirmation, and its significance is unknown. The following is, however, clear: osteoclasts *in vitro* respond to changes in $[Ca^{2+}]_o$ with increases in $[Ca^{2+}]_i$; high $[Ca^{2+}]_o$ suppress bone resorption (10); and local $[Ca^{2+}]$ in bone during active resorption may reach concentrations as high as 40 mM (44). Thus, $[Ca^{2+}]_o$, potentially via CaR activation, may regulate osteoclast function.

Studies by Quarles *et al.* (13) and Yamaguchi *et al.* (14) showed that changes in $[Ca^{2+}]_o$ and CaR agonists modulate DNA synthesis and chemotaxis in osteoblast-like MC3T3-E1 cells. Membrane CaRs were proposed by both groups to mediate the responses of osteoblasts to $[Ca^{2+}]_o$ (13, 14). There is controversy, however, regarding the molecular identity of these receptors. Sequences homologous to known CaRs, were identified by Yamaguchi *et al.* (14). Quarles *et al.* (13), however, did not detect CaR sequences by RT-PCR. The reasons for these differences may be methodologic (14). Our studies to assess CaR expression using immunocytochemistry, *in situ* hybridization, and immunoblotting support the idea that molecules homologous to known parathyroid and kidney CaRs are present in bone (16, 17).

Although full-length cDNAs encoding chondrocyte or osteoblast CaRs have not yet been isolated, our data underscore the biochemical and functional similarities between such putative receptors and known CaRs. *In situ* hybridization with a CaR probe indicated the presence of transcripts in cartilage and bone with homology to known CaRs. RT-PCR demonstrated a product whose sequence was highly homologous to CaR cDNAs identified in other tissues. Antisera raised against intracellular and extracellular epitopes of the bovine parathyroid CaR revealed similar staining patterns in both rat and bovine cartilage and bone sections. Western blotting suggested interesting biochemical differences between CaRs in cartilage and bone and those in the parathyroid. Variations in the number and sizes of CaR proteins by Western blotting were also reported in UMR-106, SaOS-2, and MC3T3-E1 cells (14, 45). Variable degrees of glycosylation could explain the differences in molecular weights among these putative CaRs. Alternatively spliced variants of the CaR may be expressed in osteogenic and chondrogenic cells similar to those reported in keratinocytes (26). Molecular cloning of full-length CaR cDNAs in cartilage and bone will be required to address these issues. The present studies, taken together, begin to address potentially key aspects of the control of chondrogenic and skeletal function that may be subject to local regulation by extracellular Ca^{2+}.

References

1. **Boskey AL** 1992 Mineral-matrix interactions in bone and cartilage. Clin Orthop 281:244–74
2. **Tuan RS** 1991 Ionic regulation of chondrogenesis. In: Hall BK, Newman SA (eds) Cartilage: Molecular Aspects. CRC Press, Inc., Boca Raton, CA, pp 153–178
3. **Poole AR** 1991 The growth plate: cellular physiology, cartilage assembly, and mineralization. In: Hall BK, Newman SA (eds) Cartilage: Molecular Aspects. CRC Press, Inc., Boca Raton, CA, pp 179–212
4. **Klein GL, Simmons DJ** 1993 Nutritional rickets: thoughts about pathogenesis. Ann Med 25:379–384
5. **Iannotti JP, Brighton CT, Stambough JL, Storey BT** 1985 Calcium flux and endogenous calcium content in isolated mammalian growth-plate chondrocytes, hyaline-cartilage chondrocytes, and hepatocytes. J Bone Joint Surg Am 67:113–120
6. **Bonen DK, Schmid TM** 1991 Elevated extracellular calcium concentrations induce type X collagen synthesis in chondrocyte cultures. J Cell Biol 115:1171–1178
7. **Jacenko O, Tuan RS** 1995 Chondrogenic potential of chick embryonic calvaria: I. Low calcium permits cartilage differentiation. Dev Dyn 202:13–26
8. **Wong M, Tuan RS** 1995 Interactive cellular modulation of chondrogenic differentiation *in vitro* by subpopulations of chick embryonic calvarial cells. Dev Biol 167:130–147
9. **Chang W, Tu C, Bajra R, Komuves L, Miller S, Strewler G, Shoback D** 1999 Calcium sensing in cultured chondrogenic RCJ3.1C5.18 cells. Endocrinology 140:1911–1919
10. **Zaidi M, Alam AS, Huang CL, Pazianas M, Bax CM, Bax BE, Moonga BS, Bevis PJ, Shankar VS** 1993 Extracellular Ca^{2+} sensing by the osteoclast. Cell Calcium 14:271–277
11. **Kameda T, Mano H, Yamada Y, Takai H, Amizuka N, Kobori M, Izumi N, Kawashima H, Ozawa H, Ikeda K, Kameda A, Hakeda Y, Kumegawa M** 1998 Calcium-sensing receptor in mature osteoclasts, which are bone resorbing cells. Biochem Biophys Res Commun 245:419–422
12. **Godwin SL, Soltoff SP** 1997 Extracellular calcium and platelet-derived growth factor promote receptor-mediated chemotaxis in osteoblasts through different signaling pathways. J Biol Chem 272:11307–11312
13. **Quarles LD, Hartle JE, Middleton JP, Zhang J, Arthur JM, Raymond JR** 1994 Aluminum-induced DNA synthesis in osteoblasts: mediation by a G-protein coupled cation sensing mechanism. J Cell Biochem 56:106–117

14. **Yamaguchi T, Chattopadhyay N, Kifor O, Butters Jr RR, Sugimoto T, Brown EM** 1998 Mouse osteoblastic cell line (MC3T3–E1) expresses extracellular calcium (Ca^{2+}o)-sensing receptor and its agonists stimulate chemotaxis and proliferation of MC3T3–E1 cells. J Bone Miner Res 13:1530–1538
15. **House MG, Kohlmeier L, Chattopadhyay N, Kifor O, Yamaguchi T, Leboff MS, Glowacki J, Brown EM** 1997 Expression of an extracellular calcium-sensing receptor in human and mouse bone marrow cells. J Bone Miner Res 12:1959–1970
16. **Brown EM, Gamba G, Riccardi D, Lombardi M, Butters R, Kifor O, Sun A, Hediger MA, Lytton J, Hebert SC** 1993 Cloning and characterization of an extracellular Ca^{2+}-sensing receptor from bovine parathyroid. Nature 366:575–580
17. **Brown EM, Pollak M, Riccardi D, Hebert SC** 1994 Cloning and characterization of an extracellular Ca(2+)-sensing receptor from parathyroid and kidney: new insights into the physiology and pathophysiology of calcium metabolism. Nephrol Dial Transplant 9:1703–1706
18. **Yamaguchi T, Kifor O, Chattopadhyay N, Brown EM** 1998 Expression of extracellular calcium (Ca^{2+}o)-sensing receptor in the clonal osteoblast-like cell lines, UMR-106 and SaOS-2. Biochem Biophys Res Commun 243:753–757
19. **Grigoriadis AE, Aubin JE, Heersche JN** 1989 Effects of dexamethasone and vitamin D3 on cartilage differentiation in a clonal chondrogenic cell population. Endocrinology 125:2103–2110
20. **Bidwell J, van Wijnen A, Banerjee C, Fey E, Merriman H, Penman S, Stein J, Lian J, Stein G** 1994 Parathyroid-responsive modifications in the nuclear matrix of ROS 17/2.8 rat osteosarcoma cells. Endocrinology 134:1738–1744
21. **Kirkwood KL, Dziak R, Bradford PG** 1996 Inositol trisphosphate receptor gene expression and hormonal regulation in osteoblast-like cell lines and primary osteoblastic cell cultures. J Bone Miner Res 11:1889–1896
22. **Sudo H, Kodama HA, Amagai Y, Yamamoto S, Kasai S** 1983 *In vitro* differentiation and calcification in a new clonal osteogenic cell line derived from newborn mouse calvaria. J Cell Biol 96:191–198
23. **Alini M, Marriott A, Chen T, Abe S, Poole AR** 1996 A novel angiogenic molecule produced at the time of chondrocyte hypertrophy during endochondral bone formation. Dev Biol 176:124–132
24. **Bikle DD, Ratnam A, Mauro T, Harris J, Pillai S** 1996 Changes in calcium responsiveness and handling during keratinocyte differentiation. Potential role of the calcium receptor. J Clin Invest 97:1085–1093
25. **Chang W, Pratt S, Chen T-H, Nemeth E, Huang Z, Shoback D** 1998 Coupling of calcium receptors to inositol phosphate and cyclic AMP generation in mammalian cells and *Xenopus laevis* oocytes and immunodetection of receptor protein by region-specific antipeptide antisera. J Bone Miner Res 13:570–580
26. **Oda Y, Tu CL, Pillai S, Bikle DD** 1998 The calcium sensing receptor and its alternatively spliced form in keratinocyte differentiation. J Biol Chem 273:23344–23352
27. **Shoback DM, McGhee JM** 1988 Fluoride stimulates the accumulation of inositol phosphates, increases intracellular free calcium, and inhibits parathyroid hormone release in dispersed bovine parathyroid cells. Endocrinology 122:2833–2839
28. **Garrett JE, Capuano IV, Hammerland LG, Hung BC, Brown EM, Hebert SC, Nemeth EF, Fuller F** 1995 Molecular cloning and functional expression of human parathyroid calcium receptor cDNAs. J Biol Chem 270:12919–12925
29. **Brown EM** 1993 Mechanisms underlying the regulation of parathyroid hormone secretion *in vivo* and *in vitro*. Curr Opin Nephrol Hypertens 2:541–551
30. **Chen CJ, Barnett JV, Congo DA, Brown EM** 1989 Divalent cations suppress 3′,5′-adenosine monophosphate accumulation by stimulating a pertussis toxin-sensitive guanine nucleotide-binding protein in cultured bovine parathyroid cells. Endocrinology 124:233–239
31. **de Jesus-Ferreira MC, Helies-Toussaint C, Imbert-Teboul M, Bailly C, Verbavatz JM, Bellanger AC, Chabardes D** 1998 Co-expression of a Ca^{2+}-inhibitable adenylyl cyclase and of a Ca^{2+}-sensing receptor in the cortical thick ascending limb cell of the rat kidney. Inhibition of hormone-dependent cAMP accumulation by extracellular Ca^{2+}. J Biol Chem 273:15192–15202
32. **Jobert AS, Fernandes I, Turner G, Coureau C, Prie D, Nissenson RA, Friedlander G, Silve C** 1996 Expression of alternatively spliced isoforms of the parathyroid hormone (PTH)/PTH-related peptide receptor messenger RNA in human kidney and bone cells. Mol Endocrinol 10:1066–1076
33. **Schmid TM, Bonen DK, Luchene L, Linsenmayer TF** 1991 Late events in chondrocyte differentiation: hypertrophy, type X collagen synthesis and matrix calcification. In Vivo 5:533–540
34. **Iannotti JP, Brighton CT** 1989 Cytosolic ionized calcium concentration in isolated chondrocytes from each zone of the growth plate. J Orthop Res 7:511–518
35. **Wuthier RE** 1993 Involvement of cellular metabolism of calcium and phosphate in calcification of avian growth plate cartilage. J Nutr 123:301–309
36. **Lian JB, McKee MD, Todd AM, Gerstenfeld LC** 1993 Induction of bone-related proteins, osteocalcin and osteopontin, and their matrix ultrastructural localization with development of chondrocyte hypertrophy *in vitro*. J Cell Biochem 52:206–219
37. **Pacifici M, Oshima O, Fisher LW, Young MF, Shapiro IM, Leboy PS** 1990 Changes in osteonectin distribution and levels are associated with mineralization of the chicken tibial growth cartilage. Calcif Tissue Int 47:51–61
38. **Nemeth EF, Scarpa A** 1987 Rapid mobilization of cellular Ca^{2+} in bovine parathyroid cells evoked by extracellular divalent cations. Evidence for a cell surface calcium receptor. J Biol Chem 262:5188–5196
39. **Ye C, Kanazirska M, Quinn S, Brown EM, Vassilev PM** 1996 Modulation by polycationic Ca(2+)-sensing receptor agonists of nonselective cation channels in rat hippocampal neurons. Biochem Biophys Res Commun 224:271–280
40. **Gu C, Cooper DM** 1999 Calmodulin-binding sites on adenylyl cyclase type VIII. J Biol Chem 274:8012–8021
41. **Mons N, Guillou JL, Jaffard R** 1999 The role of Ca^{2+}/calmodulin-stimulable adenylyl cyclases as molecular coincidence detectors in memory formation. Cell Mol Life Sci 55:525–533
42. **Kimmel DB, Jee WS** 1980 Bone cell kinetics during longitudinal bone growth in the rat. Calcif Tissue Int 32:123–133
43. **Miller SC, Marks Jr SC** 1982 Osteoclast kinetics in osteopetrotic (ia) rats cured by spleen cell transfers from normal littermates. Calcif Tissue Int 34:422–427
44. **Silver IA, Murrills RJ, Etherington DJ** 1988 Microelectrode studies on the acid microenvironment beneath adherent macrophages and osteoclasts. Exp Cell Res 175:266–276
45. **Yamaguchi T, Chattopadhyay N, Kifor O, Brown EM** 1998 Extracellular calcium (Ca^{2+}o)-sensing receptor in a murine bone marrow-derived stromal cell line (ST2): potential mediator of the actions of Ca^{2+}o on the function of ST2 cells. Endocrinology 139:3561–3568